Available online at www.sciencedirect.com
SCIENCE DIRECT
Catalysis Today 105 (2005) 634–640
CATALYSIS TODAY
www.elsevier.com/locate/cattod

# Structure and size effects in catalysis by immobilized nanoclusters of iron oxides

Mark V. Tsodikov [a,*], Tatiana N. Rostovshchikova [b,1], Vladimir V. Smirnov [b,1], Olga I. Kiseleva [b,1], Yuri V. Maksimov [c,2], Igor P. Suzdalev [c,2], Vladimir N. Ikorskii [d,3]

[a] *Topchiev Institute of Petrochemical Synthesis, RAS, Leninskii Prospect, 29, Moscow 119991, Russia*
[b] *Lomonosov Moscow State University, Moscow 119899, Russia*
[c] *Semenov Institute of Chemical Physics, RAS, Kosygina Street, 4, Moscow 119977, Russia*
[d] *Internatial Tomograpfy Centre SB RAS, Institutskaya Street, 3a, Novosibirsk 630090, Russia*

Available online 11 July 2005

**Abstract**

The activities of catalysts containing $\alpha$-$Fe_2O_3$ or $\gamma$-$Fe_2O_3$ nanoparticles supported on two types of silica (silica gel and layer silica) are tested in 3,4-dichlorobutene-1 isomerization and benzene alkylation by allyl chloride. $\gamma$-$Fe_2O_3$ particles supported on layer silica are the most active catalysts for both reactions. The high activity is associated with features of inverse spinel structure of $\gamma$-ferric oxide. The particle size and their location on the surface or interplane cavity of layer silica affect the catalytic activity.


*Keywords:* Catalysis; Immobilized nanoclusters; Iron oxides

## 1. Introduction

The fact that catalytic properties of metallic nanoclusters depend on cluster size is generally accepted and thoroughly studied [1]. The size effects in catalysis over metal oxide nanoclusters are still not clearly understood. The problem becomes more complicated because catalytic properties of metal oxide nanoclusters depend not only on cluster size but also on their structure. Previously, we studied structure and size effects in catalytic reactions of Cl-containing hydrocarbons that proceed over iron oxide nanoclusters supported on $SiO_2$ or stabilized in polymer matrix (polyethylene or polytetrafluoroethylene) [2–4]. Iron oxide nanoclusters are more effective and selective for the conversions of chloroolefins of allyl structure, i.e. isomerization or benzene alkylation by chloroolefins, than corresponding massive (bulk) oxides [2]. Bulk iron oxide causes mostly the oligomerization of chloroolefins while no products of the oligomerization were detected using iron oxide nanoparticles. In the presence of gaseous oxygen iron oxide nanoparticles catalyze either isomerization of 3,4-dichlorobutene-1 to *trans*-1,4-dichlorobutene-2 or benzene alkylations by allyl chloride or by 3,4-dichlorobutene-1. Allyl chloride can react with benzene like chlorohydrocarbon or olefin yielding two main products, namely $C_6H_5$–$CH_2$–CH=$CH_2$ and $C_6H_5$–$CH_2$–CHCl–$CH_3$. The reaction of 3,4-dichlorobutene-1 with benzene proceeds by the same way via breakage of C–Cl or C=C bonds. However, the lack of gaseous oxygen causes only 3,4-dichlorobutene-1 isomerization in benzene solution. This reaction also proceeds via breakage of C–Cl or C=C bonds. Without benzene, the isomerization rate is insensitive to the presence of gaseous oxygen. The following factors strongly affect the catalytic behavior of iron oxide nanoclusters: the nature of iron precursors, the structure of support or polymer matrix, the routine of pretreatment of support or polymer matrix and the total iron oxide content [2–4]. These factors control catalyst

* Corresponding author. Fax: +7 95 230 22 24.
*E-mail addresses:* tsodikov@ips.ac.ru (M.V. Tsodikov), rtn@kinet.chem.msu.ru (T.N. Rostovshchikova), maksimov@chph.ras.ru (Y.V. Maksimov), ikor@tomo.nsk.ru (V.N. Ikorskii).
[1] Fax: +7 95 932 88 46.
[2] Fax: +7 95 137 83 18.
[3] Fax: +7 38 323 31 399.

0920-5861/$ – see front matter © 2005 Elsevier B.V. All rights reserved.
doi:10.1016/j.cattod.2005.06.014

composition, nanocluster size and structure as well as catalytic activity. With the use of kinetic measurements, Mossbauer and X-ray powder diffraction studies, it has been suggested [2–4] that the formation of mixed-valence iron species can play a determining role in the catalytic conversions of chloroolefins. The delay of formation of the mixed-valence iron species seems to cause an induction period that often happens in these reactions.

The purpose of this work is to elucidate the role of iron oxide structure and particle size as well as of a nature of the support and cluster–support interactions in the formation of catalytically active systems. Two oxide systems, α-$Fe_2O_3$ and γ-$Fe_2O_3$ nanoparticles supported on silica with varied iron content, were prepared. Two types of silica supports with different structure, silica gel and activated matrix of silica with layer structure [3], were used. The activities of catalysts were tested in 3,4-dichlorobutene-1 isomerization:

$$CH_2ClCHClCH{=}CH_2 \rightleftarrows CH_2ClCH{=}CHCH_2Cl \quad (1)$$

and benzene alkylation by allyl chloride:

$$C_6H_6 + CH_2Cl\text{-}CH{=}CH_2 \rightarrow C_6H_5\text{-}CH_2\text{-}CH{=}CH_2 + HCl \quad (2a)$$

$$C_6H_6 + CH_2Cl\text{-}CH{=}CH_2 \rightarrow C_6H_5\text{-}CH_2\text{-}CHCl\text{-}CH_3 \quad (2b)$$

## 2. Experimental

### 2.1. Catalyst preparation

The catalysts with Fe content ranging 2.5–15 wt.% were prepared by the impregnation of a support with water solution of iron nitrate (type A) or with a solution of iron acetyl acetonate $Fe(acac)_3$ in toluene (type B) followed by their thermal treatment in air at $T = 400$ °C. Mesoporous silica gel (MSG, 340 $m^2/g$) and activated matrix of silica (AMS, 350 $m^2/g$) with layer structure produced by selective acidic etching of natural mineral ''vermiculite'' [5] were used as the supports.

### 2.2. Catalyst characterization

The A-type catalysts were described in detail in previous papers [2,3].

All B-type catalysts were X-ray amorphous. They were thoroughly studied by Mossbauer spectroscopy. Mossbauer spectra were recorded at the temperature range 6–300 K on a conventional gamma-resonance spectrometer with $^{57}Co(Rh)$ (room temperature) as a source. The spectra were computer-fitted using the standard programs for Mossbauer transition 3/2 → 1/2.

Magnetic properties of catalysts were studied on SQUID-magnetometer at temperatures 2–300 K in International Thomographic Center of Siberian Branch of Russian Academy of Sciences.

### 2.3. Catalytic experiments

The reactions were carried out in the presence of oxygen at 80–130 °C in the sealed ampoules; intensive stirring was used like in [2,3]. The products were analyzed by means of gas chromatography, chromatomass spectrometry and NMR ($^1H$ and $^{13}C$) spectroscopy. The main products were *trans*-1,4-dichlorobutene-2 in the isomerization (1), and $C_6H_5$–$CH_2$–CH=$CH_2$ and $C_6H_5$–$CH_2$–CHCl–$CH_3$ in the alkylation (2). For the highest reaction rate, the values of overall catalytic activity were expressed by mole of products per mole of iron in hour.

## 3. Results and discussion

### 3.1. Structural and magnetic properties

It was found in [2,3] that A/MSG catalysts with total iron content between 3 and 15 wt.% contained mainly α-$Fe_2O_3$ nanoclusters. These nanoclusters possessing rhombohedral structure showed polymodal size distribution where α-$Fe_2O_3$ clusters with average size $d \sim 10$–15 nm prevail. Besides nanoclusters α-$Fe_2O_3$, these catalysts contained also smaller clusters of γ-ferric oxide with $d \leq 5$–6 nm showing superparamagnetic behavior. With decreasing of total iron content (≤5 wt.%), the relative content of smaller clusters increased. At 15 wt.% of total iron content, magnetic clusters of non-stoichiometric magnetite with average size of $d \sim 10$ nm appear as well.

The use of $Fe(acac)_3$ as a precursor resulted in the stabilization of only small superparamagnetic γ-$Fe_2O_3$ clusters. The typical Mossbauer spectra of B-type catalysts containing 2.5 wt.% Fe are shown in Fig. 1. The results of computer fitting of the spectra are summarized in Table 1.

The $^{57}Fe$ Mossbauer spectrum in Fig. 1a was fitted to one doublet describing ''paramagnetic'' high-spin $Fe^{3+}$ site in the octahedral surroundings of $O^{2-}$ ions. The value of quadruple splitting for $Fe^{3+}$ site is typical for both isolated non-interacting ferric ions in the local polyhedron $FeO_6$ located in inorganic matrixes, polymer chains, etc., and showing significant axial distortion or for magnetic ferric oxide nanoclusters showing superparamagnetic behavior. The spectrum in Fig. 1b was fitted to one doublet of octahedral high-spin $Fe^{3+}$ site, which is similar to that in Fig. 1a and to six-line magnetic pattern that characterizes ferric ions involved to extended magnetic interactions and showing superparamagnetic behavior. The shape of magnetic hyperfine structure lines and significant line broadening ($\Gamma = 1.40$ mm/s) testify to the symmetric hyperfine

Table 1
Mossbauer parameters of the Fe sites in B/MSG catalyst with 2.5 wt.% of total iron content

| $T$ (K) | Component | $\delta$ (±0.03 mm/s) | $\Delta$ (±0.03 mm/s) | $\Gamma$ (±0.03 mm/s) | $H_{in}$ (±0.5 T) | Relative content (±5%) |
|---|---|---|---|---|---|---|
| 78 | $Fe^{3+}$ (paramagnetic) | 0.33 | 0.93 | 0.65 | – | 100 |
| 6 | $Fe^{3+}$ (paramagnetic) | 0.32 | 0.76 | 0.68 | – | 22 |
| | $Fe^{3+}$ (magnetic) | 0.29 | 0.00 | 1.40 | 45.0 | 78 |

$\delta$ is isomer shift, relative to α-Fe; $\Delta$ is quadruple shift or quadruple splitting; $\Gamma$ is line width; $H_{in}$ is internal magnetic field.

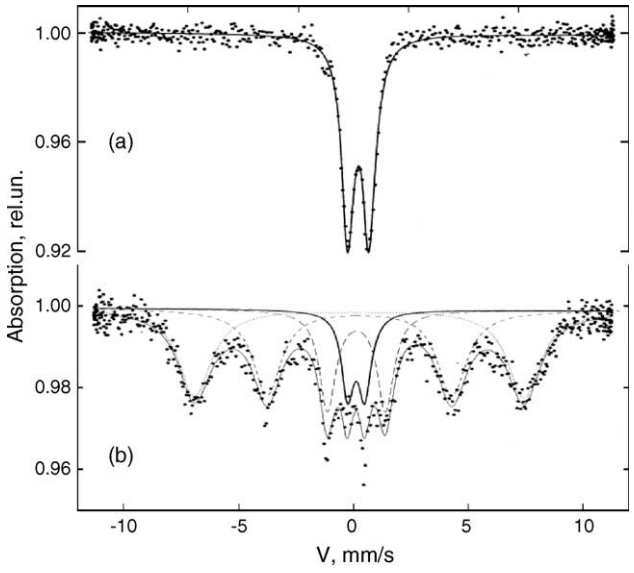


Fig. 1. Mossbauer spectra of B/MSG catalyst with 2.5 wt.% Fe at different temperatures: (a) $T = 78$ K and (b) $T = 6$ K.

field distribution around some mean value. This mean value of internal magnetic field $H_{in} \sim 45.0$ T and especially the zero value of quadruple shift indicates the cubic symmetry of γ-ferric oxide magnetic clusters. Assuming blocking temperature $T_B \sim 40$ K and using the expression for the spin–flip process of the magnetic moment in superparamagnetic nanoparticles: $\tau_s = \tau_o \exp(KV/k_BT)$, where $\tau_o$ is of the order of $10^{-10}$ s, $K$ is the effective anisotropy constant ($\sim 1.5 \times 10^5$ J/m$^3$) and $\tau_s$ is of the order of $2.5 \times 10^{-9}$ s [6], we obtain the size estimation $d \sim 2$–4 nm for γ-ferric oxide nanoclusters. Previously, γ-ferric oxide clusters of 2–3 nm obtained by thermal decomposition of ferric oxalate were studied at the temperature range 4.2–300 K [7]. At $T = 4.2$ K, clusters showed magnetic ordering while at the temperatures 4.2–78 K, they were superparamagnetic. This is very similar to the magnetic behavior of nanoclusters observed in the present work. Basing on the data [7], the average size of γ-ferric oxide nanoclusters in the B/MSG and B/AMS catalysts containing 2.5 wt.% Fe is $d \sim 3$–4 nm that is in agreement with the above estimation.

Magnetic properties of the B-type catalysts are shown in Figs. 2 and 3. Figs. 2a and 3a demonstrate magnetizations of B/MSG and B/AMS catalysts containing 2.5 wt.% Fe versus external magnetic field. In accordance with SQUID measurements, the γ-$Fe_2O_3$ nanoclusters in both catalytic systems do not have enough thermal energy at 2 K to reach a complete thermal equilibrium with the applied field during the time enough for the measurement, and thus hysteresis appears. Smaller retentivity and coercitivity for the superparamagnetic clusters of B/AMS catalyst seem to testify to smaller cluster size compared to B/MSG catalyst. For the B/AMS catalyst, the dependence of $\chi^{-1}$ versus $T$ is characterized by the sharp drop at temperature $\leq 10$ K in contrast to gentle sloping at $T \leq 50$ K for B/MSG catalyst (Figs. 2b and 3b). From the character of these curves, we may suggest a narrow size distribution in the B/AMS

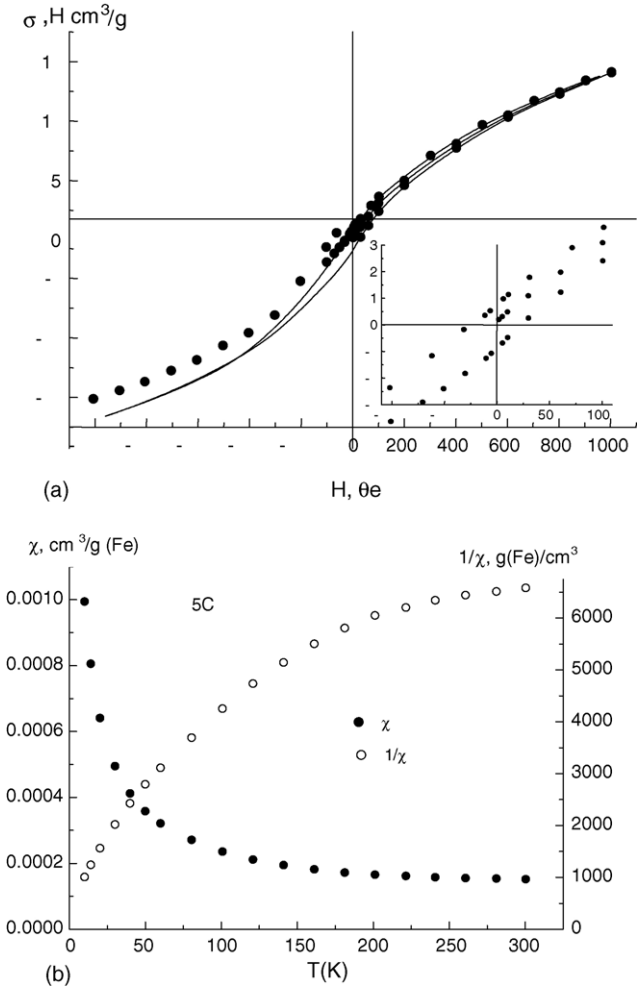


Fig. 2. Magnetic properties of B/MSG catalyst (Fe 2.5%) at 2 K: (a) dependence of magnetization vs. magnetic field, magnetization—$H$ (cm$^3$/g) (Fe), field—$\theta e$; (b) dependence of magnetic susceptibility vs. temperature, magnetic susceptibility (cm$^3$/g) (left), reverse volume of magnetic susceptibility (right).

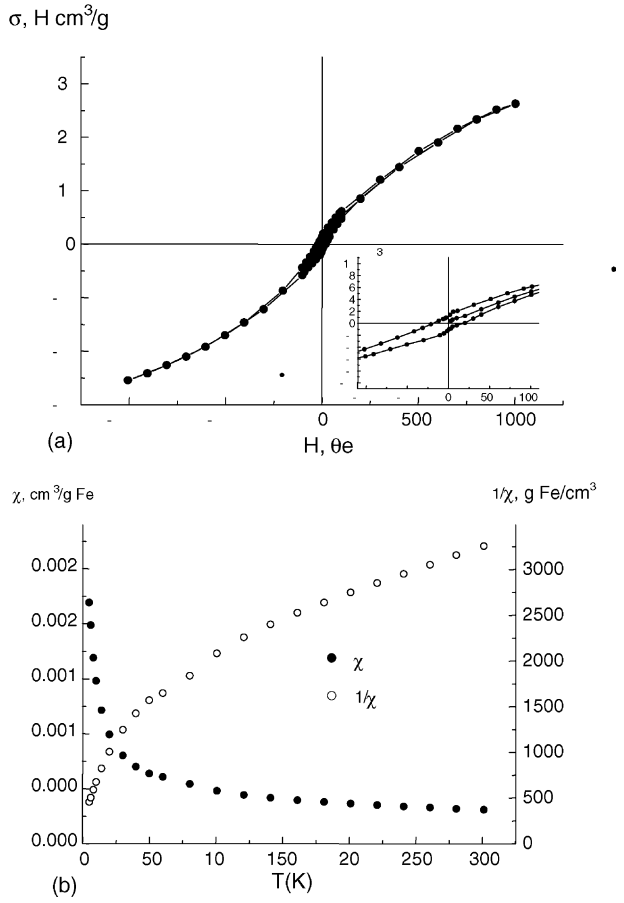


Fig. 3. Magnetic properties of B/AMS catalyst (Fe 2.5%) at 2 K: (a) dependence of magnetization vs. magnetic field, magnetization—$H$ ($cm^3/g$) (Fe), field—$\theta e$; (b) dependence of magnetic susceptibility vs. temperature, magnetic susceptibility ($cm^3/g$) (left), reverse volume of magnetic susceptibility (right).

catalyst in contrast to a broader distribution in the B/MSG catalyst. The latter conclusion is in agreement with Mossbauer results.

Fig. 4 shows room temperature Mossbauer spectra of the B-type catalysts containing 2.5% Fe/AMS, 4.5% Fe/AMS and 18% Fe/AMS. The spectrum of 2.5% Fe/AMS catalyst consisting of ''paramagnetic'' doublet with $\delta = 0.33$ mm/s and $\Delta = 0.97$ mm/s characterizes the high spin $Fe^{3+}$ ions surrounded by an octahedron of $O^{2-}$ ions and entering small superparamagnetic ferric oxide clusters. Besides $Fe^{3+}$ ions, a small amount of $Fe^{2+}$ ion is also present in the catalyst. The spectrum in Fig. 4a is practically similar to the spectrum of B-type catalyst 2.5% Fe/MSG (Fig. 1) where small superparamagnetic $\gamma$-$Fe_2O_3$ clusters are present.

The spectra of the samples 4.5% Fe/AMS and 18% Fe/AMS (Fig. 4b and c) show the presence of magnetic hyperfine structure arising from magnetically ordered $\gamma$-$Fe_2O_3$ clusters with the value of internal magnetic fields $H_{in} \sim 49.4$ T. Two facts that the onset of magnetic order in clusters occurs at room temperature and all three samples are X-ray amorphous indicate that magnetically ordered clusters have the size $d \sim 8$–$10$ nm [8]. Along with HFS lines related

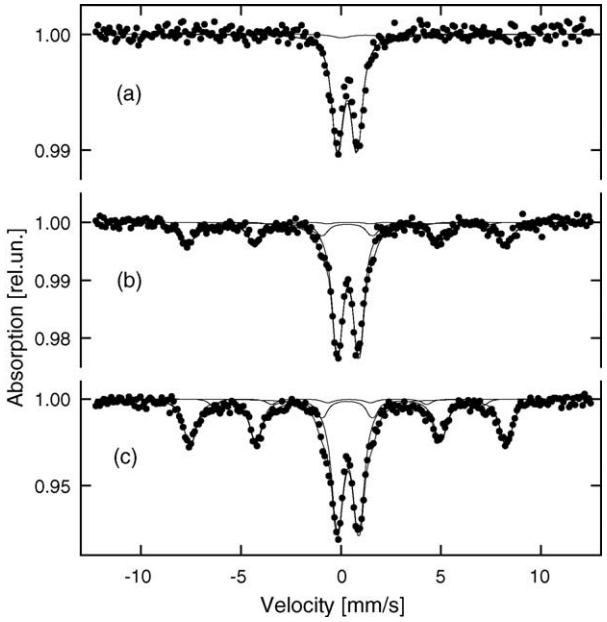


Fig. 4. Mossbauer spectra (room temperature) of B/AMS catalysts with different Fe contents: (a) 2.5%, (b) 4.5% and (c) 18%.

to magnetically ordered clusters, the spectrum in Fig. 4c contains a doublet arising from ''paramagnetic'' high-spin $Fe^{3+}$ ions that seems to belong to small $\gamma$-$Fe_2O_3$ clusters. For the catalysts 4.5% Fe/AMS and 18% Fe/AMS, the intensity ratio of HFS lines tends to growth from ~0.37 to ~0.5.

### 3.2. Catalytic properties

#### 3.2.1. Isomerization

For the A-type catalysts containing mainly $\alpha$-$Fe_2O_3$ nanoparticles, the dichlorobutene isomerization (1) proceeds via an induction period [2,3]. It has been found that the induction period decreases and the catalytic activity increases with the growth of a total iron content. For the A-type catalysts, the highest activity was observed at high iron content (15%). In this case, the catalyst contained magnetically ordered nanoclusters $\gamma$-$Fe_2O_3$ along with nanoclusters of magnetite with average size $d \sim 10$ nm. At low iron content, the A-type catalysts exhibited the greatest induction period while the catalytic activity was small [3]. These less active catalysts containing small oxide nanoclusters are stable to reduction in the reaction conditions that may be caused by the strong cluster–support interaction [9]. On the contrary, the more active catalysts containing larger in size nanoclusters are unstable to reduction. Thus, when manufacturing active and stable catalysts, it is important to create such a system that on one hand should contain labile iron oxide nanoclusters readily forming active in catalysis mixed-valence intermediates and on the other hand should be stable for the deep reduction when non-active Fe(II) compounds appear.

The best candidate satisfying the above demands seems to be the B-type catalyst prepared from $Fe(acac)_3$ as a

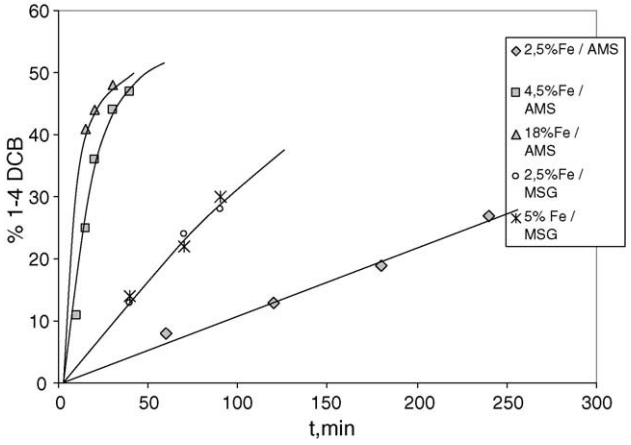


Fig. 5. Kinetic curves of 1,4-dichlorobutene-2 accumulation over B-type catalysts with different iron contents supported on silica MSG and AMS in isomerization (1) at 70 °C (3,4-dichlorobutene-1, 9 mol/l; iron, 0.003 mol/l).

precursor. Indeed, these catalysts containing γ-$Fe_2O_3$ nanoparticles showed the high activity in isomerization (1). The kinetic curves of the 1,4-dichlorobutene-2 accumulation in the presence of B-type catalysts are shown in Fig. 5. Even at 70 °C, no induction period was observed for these catalysts. Fig. 6 shows the comparison of catalytic activity of A- and B-type catalysts with different iron loading, different iron oxide and support structure. It is seen from these data that for the catalysts containing γ-$Fe_2O_3$ and α-$Fe_2O_3$, nanoclusters with the same iron loading and close cluster size the activity of the former is much higher than that of the latter. Besides iron oxide structure and size, a structure of silica affects the catalytic activity as well. Thus, for B-type catalysts, the use of MSG gives rise to more active catalysts at low iron loading, and also their activity is insensitive to iron content. Conversely, when AMS was used as a support, the growth of iron loading causes an increase of catalyst activity. The catalysts on AMS with the Fe content >4.5% are more active in catalysis compared to the catalysts on MSG.

These results permit us to propose that for catalysts with low iron loading (2.5%), the catalytically active sites may be located in the interplane of layer silica and strongly interact with matrix surface oxygen as it was described [5]. Probably, the contact between such sites and molecule of substrate is sterically hindered and the reaction rate is limited by diffusion. With the growth of iron content more than 4.5%, because of the increase of cluster size, a major part of cluster is arranged on a surface of the layer silica close to the mouth of the cavities. Thus, for B/AMS catalysts, the sharp increase of catalytic activity with the growth of iron loading can be caused by the removal of diffusion limitation. In addition, the fact that the catalysts with low iron loading and small cluster size are less active in catalysis may be due to the strong cluster–matrix interaction forcing surface oxygen of layer silica to be less labile. At the same time, with the growth both of iron loading and cluster size, more part of active surface becomes accessible to organic molecules causing an increase of catalytic activity.

### 3.2.2. Benzene alkylation

Nanosize iron oxides catalyze benzene alkylation by allyl chloride (2) at 80–110 °C. Many factors – temperature, duration of process, catalyst composition and structure – strongly affect the efficiency and selectivity of process [2]. For the A-type catalysts containing mainly α-$Fe_2O_3$, alkylation proceeded after the prolonged induction period (0.5–4.0 h), and the activity of such catalysts was not high (∼5–6 mol of products per mole of iron in hour for the best catalyst A/MSC with 12% Fe).

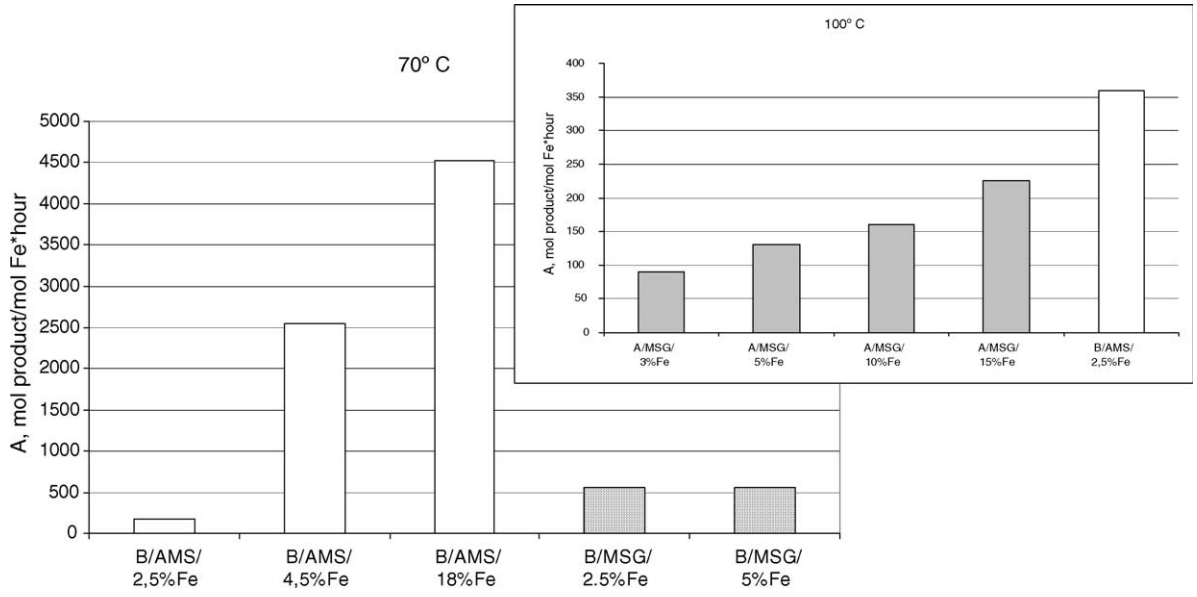


Fig. 6. Catalytic activity of A- and B-type catalysts with different iron contents on silica supports MSG and AMS in isomerization (1) at temperatures 70 and 100 °C (3,4-dichlorobutene-1, 9 mol/l; iron, 0.003 mol/l).

The B-type catalysts containing mainly small clusters of γ-$Fe_2O_3$ are more active in alkylation (2) compared to A-type catalysts. For B-type catalysts, similarly to reaction isomerization, no induction period was observed. The activity of B-type catalysts is much more higher than that of A-type catalysts. For example, 330 and 130 mol of products per mole of iron in hour were produced at 100 °C when using B-type catalysts with 4.5 and 5% Fe supported on AMS and MSG, respectively. The B-type catalysts on AMS keep their activity for several hours, whereas the activity of catalysts on MSG strongly falls down for less than an hour.

Fig. 7 demonstrates the selectivity of B-type catalysts in alkylation (2): allyl benzene (2a) prevails only at the beginning in the presence of 2.5 Fe%/AMS, then 1-phenyl-2-chloro-propane (2b) becomes dominant, which is the main product for the other catalysts. It was found in our previous work [2] that 1-phenyl-2-chloro-propane was alone product in this reaction catalyzed by typical Lewis acid—anhydrous iron (III) chloride. Thus, it may be suggested that acidic properties of the iron-contained catalysts increase under reaction conditions. Hydrogen chloride resulting in (2a) may enhance the catalyst acidity. But, as it was predetermined in particular experiments in this work, gaseous HCl only slightly affects the rate of alkylation (2) and does not react with allyl benzene to form 1-phenyl-2-chloro-propane over iron oxide catalysts. A possible way of the acidity growth is the generation of defects on the surface of iron oxide clusters in catalytic system in the course of reaction (2a) accompanied by HCl formation. The mechanism of alkylation over iron-contained catalysts will be discussed in detail in the next paper. But now we can say that there are many common features in the reactions (1) and (2) proceedings over nanosize ferric oxide catalysts through the breakage of C–Cl or C=C bonds in allyl-type chloroolefins.

The main feature of these processes is that the high catalytic activity was observed over catalysts based on layer silica and containing the nanosized clusters of γ-ferric oxide with an inverse spinal structure. Such system can be described [10] by the quasichemical equation:

$$Fe_A^{3+}[Fe^{2+}Fe^{3+}]_B O_4^{2-} \rightarrow Fe_A^{3+}[(Fe_{1-3\delta}^{2+}Fe_{1-3\delta}^{3+})Fe_{3\delta}^{3+}V_\delta]O^{2-},$$

where A and B are tetrahedral and octahedral sublattices, V a cation vacancy, ($Fe_{1-3\delta}^{2+}Fe_{1-3\delta}^{3+}$) the cations participating in Verwey double electron exchange and $\delta$ is a parameter of the non-stoichiometry changing values between 0 and 1/3 upon transition from $Fe_3O_4$ to γ-$Fe_2O_3$. Each cation vacancy removes five cations from the ''paired'' Verwey exchange, forming terminal $Fe^{3+}$=$O^{2-}$ groups. It may be suggested that the surface oxygen of the ferric oxide cluster exhibits the anion-radical behavior due to thermal electron–phonon excitation accompanied by a shift in the electron density from $O^{2-}$ to $Fe^{3+}$ by analogy with properties of vanadyl, chromyl and molebdyl groups [11,12]. Spinel structure possesses defects of two types: one of them is

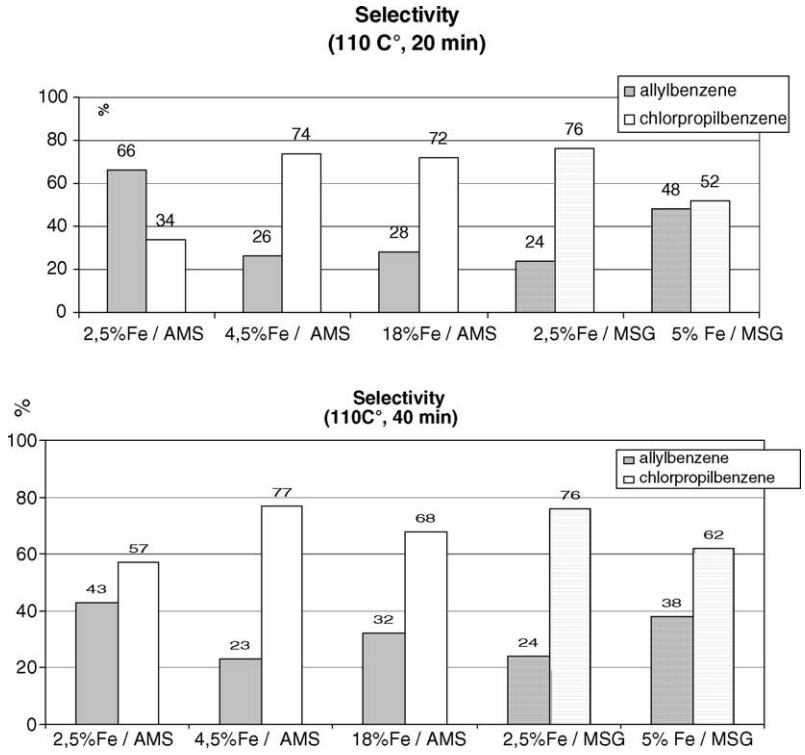


Fig. 7. Selectivity of B-type catalysts with different iron contents on two silica supports MSG and AMS in the benzene alkylation by allyl chloride (110 °C; allyl chloride, 2.6 mol/l; iron, 0.02 mol/l).

the above-mentioned cation vacancies ($\delta$) and another is anion vacancies caused by non-stoichiometric structure. Such defects can be considered as aprotic acidic sites. Both the small particle size and the layer support structure do give rise to the high concentration of such defects on an oxide surface. The combination of two type centers having ability to acidic and redox catalysis within a spinel structure may be a reason for the high catalytic activity of iron oxide–layer silica systems in the reactions studied.

## 4. Conclusions

Nanosized $\gamma$-$Fe_2O_3$ clusters supported on layer silica prepared from $Fe(acac)_3$ are active and stable catalysts for dichlorobutene isomerization and benzene alkylation by allyl chloride. The high activity is associated with features of an inverse spinel structure of $\gamma$-ferric oxide. Both the particle size and their location either on the surface or in the space of interplane of layer silica affect the catalytic activity and stability.

## Acknowledgements

The work was supported by RFBR (03-03-33104, 03-03-32029) and Program of Fundamental Researches of RAS.

## References

[1] C.R. Henry, Appl. Surf. Sci. 164 (2000) 252.
[2] T.N. Rostovshchikova, O.I. Kiseleva, G.Yu. Yurkov, S.P. Gubin, D.A. Pankratov, Yu.D. Perfil'ev, V.V. Smirnov, P.A. Chernavskii, G.V. Pankina, Moscow Univ. Chem. Bull. 56 (2001) 20.
[3] T.N. Rostovshchikova, M.V. Tzodikov, O.V. Buchtenko, V.V. Smirnov, O.I. Kiseleva, Yu.V. Maksimov, D.A. Pankratov, Russ. Chem. Bull. Int. Ed. (2), in press.
[4] T.N. Rostovshchikova, M.S. Korobov, D.A. Pankratov, G.Yu. Yurkov, S.P. Gubin, Russ. Chem. Bull. Int. Ed. (2), in press.
[5] Yu.V. Maksimov, V.V. Matveev, I.P. Suzdalev, M.V. Tsodikov, O.G. Ellert, Hyperfine Interact. 56 (1990) 1983.
[6] S. Morup, J.A. Dumesic, H. Topsque, Magnetic microcrystals, in: R.L. Cohen (Ed.), Applications of Mossbauer Spectroscopy, vol. II, Academic Press, New York, 1980, pp. 1–53.
[7] I.P. Suzdalev, V.N. Buravtsev, V.K. Imshennik, Yu.V. Maksimov, V.V. Matveev, A.V. Volynskaya, A.X. Trautwein, H. Winkler, Z. Phys. D, At. Mol. Clusters 36 (1996) 163.
[8] M.V. Tsodikov, V.Ya. Kugel, E.V. Slivinskii, G.N. Bondarenko, Yu.V. Maksimov, M.A. Alvarez, M.C. Hudalgo, J.A. Navio, Appl. Catal. A: Gen. 193 (2000) 237.
[9] P.A. Chernavskii, G.V. Pankina, V.V. Lunin, Zh. Fiz. Khim. 70 (1996) 1016.
[10] O.S. Morozova, Yu.V. Maksimov, D.P. Shashkin, P.A. Shijaev, V.A. Zhorin, O.V. Krylov, Appl. Catal. 78 (1991) 227.
[11] A.H. Gritscov, V.A. Shvets, V.B. Kazansky, Chem. Phys. Lett. 35 (1975) 511.
[12] Yu.V. Maksimov, I.P. Suzdalev, M.V. Tsodikov, V.Ya. Kugel, O.V. Bukhtenko, E.V. Slivinskii, J.A. Navio, J. Mol. Catal. A: Gen. 105 (1996) 167.